Short-Time Glassy Dynamics in Viscous Protein Solutions with Competing Interactions

P. Douglas Godfrin,[1] Steven D. Hudson,[2] Kunlun Hong,[3] Lionel Porcar,[4] Peter Falus,[4] Norman J. Wagner,[1,†] and Yun Liu[1,5,*]

[1]Center for Neutron Science, Department of Chemical and Biomolecular Engineering, University of Delaware, Newark, Delaware 19716, USA

[2]Polymers and Complex Fluids Group, NIST, Gaithersburg, Maryland 20899, USA

[3]Center for Nanophase Materials and Sciences, Oak Ridge National Laboratory, Oak Ridge, Tennessee 37831, USA

[4]Institut Laue-Langevin, 71 avenue des Martyrs, CS 20156, 38042 Grenoble cedex 9, France

[5]Center for Neutron Research, NIST, Gaithersburg, Maryland 20899, USA

(Received 25 May 2015; revised manuscript received 5 October 2015; published 24 November 2015)

The glass transition of colloidal dispersions interacting with both a short-ranged attraction and long-ranged repulsion is studied using highly purified lysozyme solutions. Newtonian liquid behavior is observed at all conditions while measurements of the dynamics in the short-time limit show features typical of glassy colloidal systems at high protein concentrations. This interesting behavior is due to the competition of the attraction and repulsion that produces a heterogeneous microstructure only at intermediate range length scales. The results demonstrate that theories for the macroscopic properties of systems with competing interactions need to include intermediate range order.

DOI: 10.1103/PhysRevLett.115.228302 PACS numbers: 82.70.Dd, 64.70.pv, 64.75.Xc, 87.15.km

Dispersions with both a short-ranged attraction and a long-ranged repulsion (SALR) are of fundamental interest as a result of the significant diversity of spontaneously formed structures (i.e., phase behavior) due to the competition of the two potential features. The range of the attraction can be varied to introduce different types of phases [1–6]. The combination of a long-ranged repulsion with a short-ranged attraction has been demonstrated to cause the formation of equilibrium cluster fluids [1,4,7–11]. While clusters in SALR systems have been observed in systems of nanoparticles in polymer composites [12] and solutions with polymer depletants [1,7] as well as membrane proteins [13], recent work has associated cluster formation with large viscosities in highly concentrated lysozyme [11] and monoclonal antibody [14] formulations, making these types of interactions relevant to the biopharmaceutical industry.

The structure and dynamics of concentrated protein solutions have been investigated extensively [7,9–11, 14–16]. In particular, the phase diagrams of globular protein solutions with pure short-ranged attraction have been widely studied at large salt concentrations [17,18]. For solutions with low salt concentrations, the presence of additional repulsion is known to shift the liquid-liquid coexistence region of an attractive fluid to lower temperatures T [3,5], and the percolation transition to smaller volume fractions ϕ [19]. For most protein systems, the range of the short-ranged attraction is only a fraction of the particle diameter [10,17]. In these cases, a recent study has demonstrated the intricate relation between the equilibrium phase behavior of systems with purely short-ranged attraction and those with SALR interactions [5]. Long-ranged repulsive forces in SALR systems serve to frustrate particle association leading to intermediate range order (IRO) [5,10]. The presence of the IRO is typically observed by the appearance of a low-Q peak in the interparticle structure factor, and is a general phenomenon of competing interactions reflecting a special arrangement of particles at the intermediate range length scale [5,10]. At low concentrations, the formation of clustered fluids is an extreme example of the IRO, indicating the ordering of clusters with a preferred size [5]. However, at high particle concentrations, the size of many clusters is so large that the IRO is simply an internal structure of individual clusters [19].

In addition to the rich equilibrium phase behavior, there is also strong interest in studying dynamical arrest transitions in systems with competing interactions. However, even for purely short-ranged attractive colloidal systems, the physical mechanism of the attraction induced dynamical arrest is a topic of debate [20–22]. The addition of a long-ranged repulsion to a short-ranged attractive system presents some new features of dynamical arrest transitions. A recent study of micrometer colloidal particles showed that dynamical arrest in suspensions of SALR systems can be determined through the observation of a greatly reduced diffusivity [4]. However, the attraction strength induced by the depletion attraction in this study is much stronger than that of most protein systems [4,10,18]. Thus, it remains unclear how dynamic state diagrams may change for protein dispersions. To explore this, we systematically probe the structure and dynamics of a model protein dispersion (lysozyme) with competing interactions over a wide range of volume fractions and temperatures. Very interestingly, we observed the transition to a localized glassy behavior at relatively high concentrations while the

dispersion remains as a Newtonian liquid over macroscopic length and time scales. Further, we show this localized dynamical arrest is driven by the formation of the intermediate range order.

Lysozyme solutions ranging in concentration from 10 mg/ml ($\phi \approx 0.008$) to 480 mg/ml ($\phi \approx 0.345$) are prepared. The volume fraction is calculated using the skeleton density of lysozyme ($\rho_0 = 1.395$ g/ml) [23] to be consistent with previous studies [9,10,18]. (Estimation of ϕ by considering a hydration layer [24] only changes the values of ϕ without affecting our conclusions.) The surface charge is consistently between 9 and 10 as the pH value is only slightly varied around 5 [25,26]. Efforts have been made to minimize the ion concentration in solutions to maximize the strength and range of repulsion [27]. Hence, even though samples at 480 mg/ml can form crystals after long incubation periods, the long-ranged repulsion stabilizes the protein during all of our experiments. Viscosity is determined using a microcapillary viscometer [28] to avoid air-water interfacial effects [29]. Lysozyme solution structures and short-time dynamics are characterized using small angle neutron scattering (SANS) and neutron spin echo (NSE), respectively, performed at the D22 and IN15 in the Institut Laue–Langevin in Grenoble, France and at the NGB30SANS in the NIST Center for Neutron Research in Gaithersburg, MD, USA. Any changes in the effective protein interactions with solution conditions are explicitly accounted for by fitting SANS data with appropriate integral equation theories [30] with the hard sphere double Yukawa potential [31].

A summary of the specific viscosity is provided in Fig. 1(a) relative to the expectations for hard sphere (HS) dispersions. The viscosity seems to qualitatively agree with the trend of HS systems at low volume fractions. However, with increasing lysozyme concentration ($\phi > 0.15$) the viscosity increases much more rapidly. The dramatic rise in viscosity when decreasing the temperature is due to an increase in the strength of the attraction between lysozyme proteins [10,11]. At the highest concentration (480 mg/ml or $\phi = 0.345$) the lysozyme solution is roughly 10 times more viscous than a HS fluid at 50 °C and decreasing the temperature to 5 °C further raises the viscosity by 2 orders of magnitude. By estimating the interparticle potential using SANS [10], we have calculated the viscosity as a function of the volume fraction using the existing theoretical framework [32]. However, it fails to reproduce the viscosity at large concentrations, which will be discussed in detail in a future paper.

Despite the high viscosities, Fig. 1(b) shows that lysozyme solutions behave as a Newtonian fluid under all conditions. The range of shear rates ($10\ \mathrm{s}^{-1} < \dot{\gamma} < 10^5\ \mathrm{s}^{-1}$) varied for each sample due to the variation in the sample viscosity and limits of pressure drop supplied [28]. Regardless, all data sets are well within the zero-shear limit of $\mathrm{Pe} = 3\pi\eta_s\sigma^3\dot{\gamma}/4k_BT \ll 1$, where η_s is the solvent viscosity and $\sigma = 30.7$ Å is the particle diameter. The highest Pe number (at low concentrations) only approached $\mathrm{Pe} \approx 2 \times 10^{-3}$. The characteristic time for protein diffusion is taken as the time for Brownian diffusion distance on the order of the particle size [4], $t_D = 3\pi\eta_s\sigma^3/4k_BT$, which is roughly 25 ns. The characteristic time scale probed by the viscosity measurements is about 5 orders of magnitude slower than the time scale of the protein diffusion. Therefore, the specific viscosities in Fig. 1(a) are representative of long-time structural rearrangement.

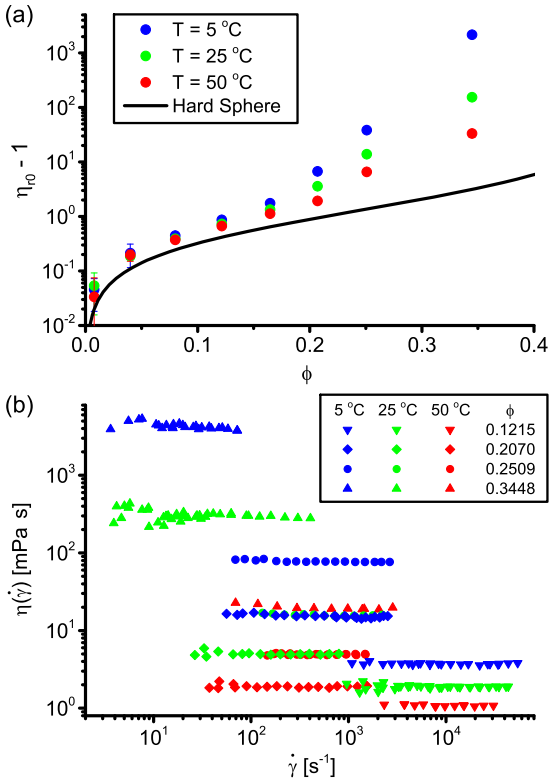

FIG. 1 (color online). (a) Specific viscosities (symbols) in the zero-shear limit are plotted as a function of protein volume fraction at three temperatures relative to HS predictions (line) [33]. (b) Solution viscosities are plotted as a function of the shear rate for selected volume fractions.

Typically, for systems of colloidal particles with purely attractive interactions in either a gel or glass state, subdiffusive behavior persists at long time ($t \gg t_D$). Also, the associated mean squared displacement (MSD) of particles becomes very small at $t \sim t_D$ [34]. These two criteria have been used extensively to identify gelation or glass transitions [4,34–36]. NSE can measure the intermediate scattering function at a relatively large wave vector, or q value, such that NSE can be used to estimate the MSD of concentrated protein solutions at $q\sigma/2 > 1$, similar to the method used in dynamic light scattering [37]. The MSD, $\langle R^2 \rangle$, at a given large q value can be described as $\langle R^2 \rangle = -(6/q^2)\ln[S(q,t)]$.

The MSD of lysozyme samples estimated using the average values of the MSD obtained through the

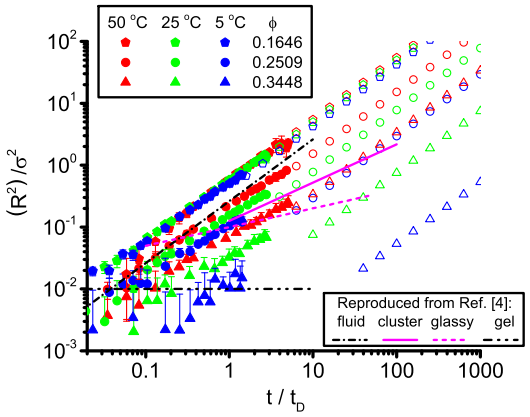

FIG. 2 (color online). The normalized mean squared displacement of lysozyme samples at short-time (filled symbols) and long-time (open symbols) are plotted as a function of normalized time. Also shown are previous results for a system with micrometer sized colloidal particles (lines) [4] representative of fluid, cluster, glassy, and gel states. Error bars represent one standard deviation.

intermediate scattering functions for $1.54 < q\sigma/2 < 2.46$ are provided in Fig. 2 (solid symbols) with respect to lines representative of fluid, cluster, glassy, and gel states that are reported previously for samples with 1.95 μm diameter PMMA particles with SALR interactions [4]. Despite the large differences in the particle size and the time scale of the measurement techniques, the normalized time ranges are similar for both lysozyme and PMMA particles [4]. The normalized MSDs of lysozyme samples at high ϕ and low T are well below the MSDs of glassy and gel samples reported previously for colloidal systems with SALR interactions [4]. This indicates that at the local length scale, lysozyme proteins in these samples have glassylike behavior. Interestingly, for the highest concentration sample at 5 °C, the MSD is similar to the values in a glassy colloidal system with only short-ranged attraction [38], and a hard sphere dispersion in a glass state measured by dynamic light scattering [37].

At times $t/t_D < 1$, which represents the short-time limit [39–41], all samples follow a power law expected for diffusive motion. At sufficiently low volume fractions ($\phi = 0.1646$), the data remain diffusive for times beyond t_D at all temperatures. However, for $\phi \geq 0.2$, the power law exponent drops below one for $t/t_D > 1$, becoming subdiffusive with decreasing temperature. These conditions correspond with the regime in Fig. 1 where the specific viscosity increases significantly. This subdiffusive behavior becomes more obvious when compared to the estimated MSD in the long-time limit.

The long-time self-diffusion coefficient can be estimated using the zero-shear viscosity according to a generalized Stokes-Einstein equation, $(D_L/D_0) \approx (1/\eta_{r0})$. Hence, the normalized long-time MSD can be approximated by $6t/(t_D\eta_{r0})$. The resulting MSDs estimated from capillary viscometry experiments are shown as open symbols in Fig. 2 with the MSDs obtained directly from NSE (filled symbols with the same conditions as the corresponding open symbols). Remarkably, although estimation of the long-time MSD using η_{r0} based on the generalized Stokes-Einstein relation is usually considered to be only qualitatively correct for relatively concentrated samples, the short and long time MSDs overlap almost perfectly in the limit of low ϕ and high T, which is consistent with a previous study where the long-time diffusivity is experimentally measured with NMR [10]. However, in the other extreme of high ϕ and low T, the long-time MSD shows clear deviations from the behavior of the MSD at the short-time limit. The discontinuity is consistent with the onset of a nonergodic plateau, and thus, the onset of localized glassy dynamics at some time $t > t_D$.

For glassy states in HS systems, particles diffuse within individual cages and therefore, remain mobile over short times [42]. However, the cages themselves are unable to rearrange leading to restricted long-time motion and a divergence of zero-shear viscosity. Thus, the relation between the solution viscosity and D_S provides a measure of the congruence between the long-time and short-time dynamic behavior. For our samples, we can estimate the diffusion coefficient in the short-time limit D_S from the MSD for the data points at $t < 25$ ns. (See the Supplemental Material for details [43].) The correlation of these two parameters is provided in Fig. 3 for lysozyme samples (solid circles), and compared with that reported for HS systems (lines), which allows the direct comparison of HS and SALR systems. Because HS systems only interact by excluded volume effects, such jammed microstructures only form at high volume fractions ($\phi \geq 0.57$) [33]. The SALR interactions cause an early onset of localized glassy behavior at $\phi \approx 0.3$.

Most notable from Fig. 3 is the lack of an apparent divergence in the lysozyme solutions' zero-shear viscosity with respect to the short-time diffusivity. At high

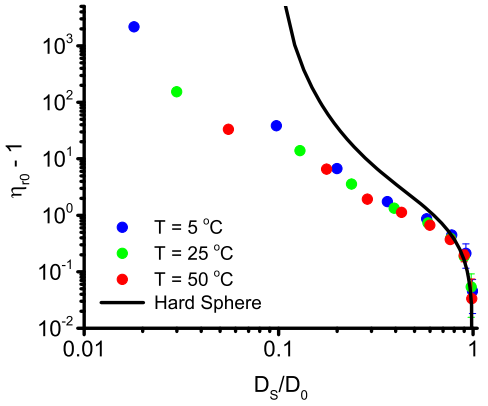

FIG. 3 (color online). The specific viscosity of lysozyme is plotted as a function of short-time self-diffusivity (symbols) relative to calculations for HS fluids (solid line).

temperature and low volume fractions, lysozyme solutions follow the HS expectations of viscosity when plotted as a function of D_S. At small D_S (large concentrations), the specific viscosity of lysozyme solutions is smaller than that of a HS system with the same value of D_S/D_0. This indicates that the long-time diffusion coefficient D_L, which is approximately inversely proportional to the relative viscosity, is faster in the lysozyme solutions as compared to a HS system. These results show that the microstructure resulting from SALR interactions is more conducive to large scale structural rearrangement.

The clear deviation from the HS behavior is due to the unique IRO structure caused by the SALR interactions that can be examined by the IRO peak evident in the solution structure factor $S(q)$. Figure 4 shows $S(q)$ extracted from SANS by normalizing scattering intensities to the data of a dilute sample. An IRO peak is observed at 5 °C for all volume fractions studied, which is consistent with the increased viscosity at this temperature. While the length scale of the IRO peak is associated with distances between locally dense regions, this localized dense packing leads to significant space with smaller protein density between dense regions on the same length scale [5]. Thus, the formation of IRO peaks in $S(q)$ indicates a unique localization of proteins at the IRO length scale. A decrease in the IRO peak intensity at high temperatures indicates the loss of intermediate range order. Hence, the system becomes more uniformly distributed, which corresponds with a decrease of the viscosity. Eventually, at high enough temperature, the attractive forces are insufficient to induce intermediate range particle localization, represented by the transition from a peak to a weak shoulder that then disappears. Therefore, for a given volume fraction, the growth of the IRO peak with decreasing temperature demonstrates a preference for strong particle localization that significantly reduces the short-time mobility. Simultaneously, IRO introduces void space available to proteins, making the exchange between local environments easier on the longer time scale.

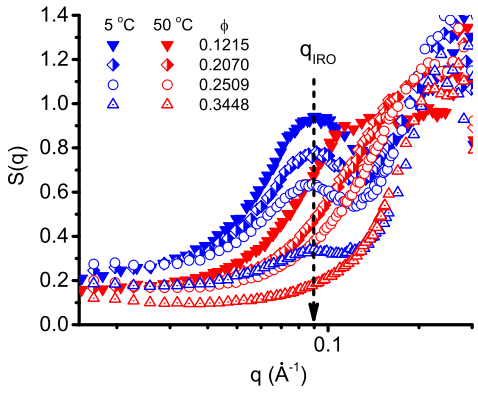

FIG. 4 (color online). Structure factors obtained from SANS are plotted for several sample conditions, indicating the formation of IRO peaks at the same q value (q_{IRO}) shown by the dotted line.

The localized heterogeneous density distribution can be also understood from the MSD. For the sample at the largest concentration and lowest temperature, the $\langle R^2 \rangle$ at $t/t_D \approx 1$ is roughly about $0.01\sigma^2$. This can be used to approximately estimate the order of magnitude of the cage size, which is about 0.1σ. (Note that the accurate cage size is typically estimated at the measurement time when the non-Gaussian factor reaches a maximum.) The small cage size is consistent with high local density driven mainly by the short-ranged attraction.

On the other hand, at the large length scale, the small values of $S(q)$ at low q region, as shown in Fig. 4, indicate that the long-ranged repulsion makes the solution structure very uniform over distances larger than the IRO length scale. Thus, the heterogeneous density distribution is localized at length scales smaller than or comparable to the IRO length scale. This is different from the commonly studied colloidal gel systems, which form a heterogeneous density distribution on a much larger length scale that tends to expand to the entire system. The lower resistance to shear flow in SALR systems relative to HS fluids with an equivalent short-time self-diffusivity arises from this localized heterogeneous particle distribution that opens a sufficient free volume for the protein network to rearrange and relax macroscopically. Such a microstructure contains a diverse landscape of local environments that will influence the mobility of individual particles in a nontrivial way.

In conclusion, while lysozyme is an extensively studied system, this work is the first to clearly demonstrate the nontrivial impact of the IRO on the onset of the localized glassy behaviors, and on the dynamics and viscosity of systems with both a short-ranged attraction and a long-ranged repulsion by providing accurate measurements of viscosity, short-time self-diffusivity, and interparticle structures over a large range of concentrations and temperatures. The existence of IRO introduces localized heterogeneous density distributions at the length scale comparable to that extracted from the IRO peak position. Over length scales larger than that of the IRO, the system is relatively uniform, but the locally large packing fraction of proteins leads to localized glassy motions. Despite the significantly slow local motion, the void space associated with the IRO enables diffusive motion at long-time scales that keeps the solutions in a macroscopic fluid state. This behavior is in contrast to protein samples without long-ranged repulsion at similar ϕ and T by adding large amount of salts to the solutions, which show either phase separation or gelation with increasing strength of attraction [18].

The experimental evidence shown here highlights the importance of both structure and dynamics corresponding to the IRO length scale in understanding the transport properties of fluids with competing potential features. Our results compliment an earlier study of the SALR systems using large micrometer sized colloidal particles, where the attraction strength between the particles is significantly

larger than that between lysozyme proteins [4]. Combining our results with the previous study provides a comprehensive picture of the effect of SALR interactions on the gel and glass transitions in many colloidal systems.

This work utilized facilities supported in part by the National Science Foundation under Agreement No. DMR-0944772. The authors acknowledge the support of Cooperative Agreements No. 70NANB12H239 and No. 70NANB10H256 from NIST, U.S. Department of Commerce. The samples were purified at CNMS, supported by the Scientific User Facilities Division, Office of Basic Energy Sciences, U.S. Department of Energy.

*yunliu@nist.gov
†wagnernj@udel.edu

[1] A. I. Campbell, V. J. Anderson, J. S. van Duijneveldt, and P. Bartlett, Phys. Rev. Lett. **94**, 208301 (2005).
[2] A. J. Archer, D. Pini, R. Evans, and L. Reatto, J. Chem. Phys. **126**, 014104 (2007).
[3] J. C. F. Toledano, F. Sciortino, and E. Zaccarelli, Soft Matter **5**, 2390 (2009).
[4] C. L. Klix, C. P. Royall, and H. Tanaka, Phys. Rev. Lett. **104**, 165702 (2010).
[5] P. D. Godfrin, N. E. Valadez-Pérez, R. Castañeda Priego, N. J. Wagner, and Y. Liu, Soft Matter **10**, 5061 (2014).
[6] B. Ruzicka, L. Zulian, E. Zaccarelli, R. Angelini, M. Sztucki, A. Moussaid, and G. Ruocco, Phys. Rev. Lett. **104**, 085701 (2010).
[7] A. Stradner, H. Sedgwick, F. Cardinaux, W. C. K. Poon, S. U. Egelhaaf, and P. Schurtenberger, Nature (London) **432**, 492 (2004).
[8] F. Sciortino, S. Mossa, E. Zaccarelli, and P. Tartaglia, Phys. Rev. Lett. **93**, 055701 (2004).
[9] L. Porcar, P. Falus, W.-R. Chen, A. Faraone, E. Fratini, K. Hong, P. Baglioni, and Y. Liu, J. Phys. Chem. Lett. **1**, 126 (2010).
[10] Y. Liu, L. Porcar, J. Chen, W.-r. Chen, P. Falus, A. Faraone, E. Fratini, K. Hong, and P. Baglioni, J. Phys. Chem. B **115**, 7238 (2011).
[11] F. Cardinaux, E. Zaccarelli, A. Stradner, S. Bucciarelli, B. Farago, S. U. Egelhaaf, F. Sciortino, and P. Schurtenberger, J. Phys. Chem. B **115**, 7227 (2011).
[12] J. S. Meth, S. G. Zane, C. Chi, J. D. Londono, B. A. Wood, P. Cotts, M. Keating, W. Guise, and S. Weigand, Macromolecules **44**, 8301 (2011).
[13] P. A. Mulheran, D. Pellenc, R. A. Bennett, R. J. Green, and M. Sperrin, Phys. Rev. Lett. **100**, 068102 (2008).
[14] E. J. Yearley, P. D. Godfrin, T. Perevozchikova, H. Zhang, P. Falus, L. Porcar, M. Nagao, J. Curtis, P. Gawande, R. Taing, I. E. Zarraga, N. J. Wagner, and Y. Liu, Biophys. J. **106**, 1763 (2014).
[15] F. Roosen-Runge, M. Hennig, F. Zhang, R. M. J. Jacobs, M. Sztucki, H. Schober, T. Seydel, and F. Schreiber, Proc. Natl. Acad. Sci. U.S.A. **108**, 11815 (2011).
[16] W. Doster and S. Longeville, Biophys. J. **93**, 1360 (2007).
[17] D. Rosenbaum, P. C. Zamora, and C. F. Zukoski, Phys. Rev. Lett. **76**, 150 (1996).
[18] F. Cardinaux, T. Gibaud, A. Stradner, and P. Schurtenberger, Phys. Rev. Lett. **99**, 118301 (2007).
[19] N. E. Valadez-Pérez, R. Castañeda Priego, and Y. Liu, R. Soc. Chem. Adv. **3**, 25110 (2013).
[20] A. P. R. Eberle, N. J. Wagner, and R. Castañeda Priego, Phys. Rev. Lett. **106**, 105704 (2011).
[21] N. E. Valadez-Pérez, Y. Liu, A. P. R. Eberle, N. J. Wagner, and R. Castañeda-Priego, Phys. Rev. E **88**, 060302(R) (2013).
[22] G. Foffi, C. De Michele, F. Sciortino, and P. Tartaglia, Phys. Rev. Lett. **94**, 078301 (2005).
[23] K. Gekko and H. Noguchi, J. Phys. Chem. **83**, 2706 (1979).
[24] B. Halle, Phil. Trans. R. Soc. B **359**, 1207 (2004).
[25] S. A. Allison and V. T. Tran, Biophys. J. **68**, 2261 (1995).
[26] M. Boncina, J. Rescic, and V. Vlachy, Biophys. J. **95**, 1285 (2008).
[27] Ç. Mecitoğlu, A. Yemenicioğlu, A. Arslanoğlu, Z. S. Elmaci, F. Korel, and A. E. Çetin, Food research international **39**, 12 (2006).
[28] S. D. Hudson, P. Sarangapani, J. A. Pathak, and K. B. Migler, J. Pharm. Sci. **104**, 678 (2015).
[29] V. Sharma, A. Jaishankar, Y.-C. Wang, and G. H. McKinley, Soft Matter **7**, 5150 (2011).
[30] J. M. Kim, R. Castañeda Priego, Y. Liu, and N. J. Wagner, J. Chem. Phys. **134**, 064904 (2011).
[31] Y. Liu, W.-R. Chen, and S.-H. Chen, J. Chem. Phys. **122**, 044507 (2005).
[32] J. F. Brady, J. Chem. Phys. **98**, 3335 (1993).
[33] W. B. Russel, N. J. Wagner, and J. Mewis, J. Rheol. **57**, 1555 (2013).
[34] E. Zaccarelli, J. Phys. Condens. Matter **19**, 323101 (2007).
[35] F. Sciortino, Nat. Mater. **1**, 145 (2002).
[36] E. Zaccarelli, S. V. Buldyrev, E. La Nave, A. J. Moreno, I. Saika-Voivod, F. Sciortino, and P. Tartaglia, Phys. Rev. Lett. **94**, 218301 (2005).
[37] W. van Megen, T. C. Mortensen, S. R. Williams, and J. Müller, Phys. Rev. E **58**, 6073 (1998).
[38] C. P. Royall, S. R. Williams, T. Ohtsuka, and H. Tanaka, Nat. Mater. **7**, 556 (2008).
[39] A. J. Banchio and G. Nägele, J. Chem. Phys. **128**, 104903 (2008).
[40] A. J. Banchio, J. Bergenholtz, and G. Nägele, Phys. Rev. Lett. **82**, 1792 (1999).
[41] A. J. Banchio, G. Nagele, and J. Bergenholtz, J. Chem. Phys. **113**, 3381 (2000).
[42] T. G. Mason and D. A. Weitz, Phys. Rev. Lett. **75**, 2770 (1995).
[43] See Supplemental Material at http://link.aps.org/supplemental/10.1103/PhysRevLett.115.228302 for the details of extracting self-diffusion coefficients from NSE data, a comparison of short and long time self-diffusion coeffcients, and a list of SANS fitting parameters.